JSES International 8 (2024) 714–718

Contents lists available at ScienceDirect

JSES International

journal homepage: www.jsesinternational.org

Evaluation of glenoid morphology and bony Bankart lesion in shoulders with traumatic anterior instability using zero echo time magnetic resonance imaging

Takayuki Oishi, MD, PhD[a], Atsushi Tasaki, MD, PhD[a,*], Shota Mashimo, PT, MPH[b], Michiru Moriya, MD[a], Daisuke Yamashita, MD[a], Taiki Nozaki, MD, PhD[c], Nobuto Kitamura, MD, PhD[a], Yutaka Inaba, MD, PhD[d]

[a]*Department of Orthopedic Surgery, St. Luke's International Hospital, Tokyo, Japan*
[b]*Department of Rehabilitation, St. Luke's International Hospital, Tokyo, Japan*
[c]*Department of Radiology, Keio University School of Medicine, Tokyo, Japan*
[d]*Department of Orthopedic Surgery, Yokohama City University, Yokohama, Japan*

ARTICLE INFO

Keywords:
Zero echo time magnetic resonance imaging
Bankart lesion
Glenoid bone loss
Anterior instability
Computed tomography
Diagnostic ability

Level of evidence: Level III; Diagnostic Study

Background: Preoperative computed tomography (CT) evaluation of bone morphometry aids in determining treatment strategies for shoulder instability. The use of zero echo time (ZTE) sequence in magnetic resonance imaging (MRI), a new bone cortex imaging technique, may help reduce radiation exposure and medical costs. Therefore, this study aimed to evaluate the glenoid morphology and detect the presence of bony Bankart lesion using ZTE MRI in shoulders with anterior instability and compare its diagnostic accuracy with that of CT.

Methods: Thirty-six patients (36 shoulders) with anterior instability who underwent preoperative CT and MRI examinations between April 2019 and October 2021 were retrospectively analyzed. The percentages of glenoid bone defects on 3-dimensional (3D) CT and ZTE images were determined, and the correlation between these percentages was evaluated. The number of cases with bony Bankart lesion on CT and 2 types of ZTE (3D and CT-like) images was determined, and the diagnostic accuracy of ZTE for detecting bony Bankart lesion was assessed, with CT as the gold standard. Patients with bony Bankart lesion on CT images were divided into 2 groups based on whether the lesion was detectable on 3D ZTE or CT-like images. The longer diameters of bony Bankart lesion were compared between the groups.

Results: The median percentage of glenoid bone loss was 12.1% (range, 1.3%-45.9%) and 12.3% (range, 0%-46.6%) on 3D CT and 3D ZTE images, respectively. The Spearman's rank correlation coefficient was 0.89. Bony Bankart lesion was detected in 18, 13, and 8 shoulders of the 36 patients on CT, 3D ZTE, and CT-like images, respectively. The overall diagnostic accuracy of the CT-like and 3D ZTE images for detecting bony Bankart lesion was 86.1% and 72.2%, respectively. A significant difference was observed between the groups with and without bony Bankart lesion on CT-like images in terms of the long diameter of the bone fragments on CT ($P < .01$).

Conclusion: ZTE MRI demonstrated high reproducibility for the evaluation of glenoid bone defect in shoulders with anterior instability. Although no significant difference in the measurement was observed compared with that on CT, the ability of ZTE MRI to delineate bone Bankart lesion remains limited.

The bony morphology of the glenoid has a significant impact on the clinical outcomes of patients with traumatic shoulder instability.[3] The presence of a bone defect of > 25% of the transverse diameter of the glenoid results in residual instability of the shoulder joint after Bankart repair.[5] Bony Bankart lesion

The Research Ethics Committee of St. Luke's International University approved this cross-sectional diagnostic study (No. 18-R022).

*Corresponding author: Atsushi Tasaki, MD, PhD, Department of Orthopedic Surgery, St. Luke's International Hospital, 9-1 Akashi-cho, Chuo-ku, Tokyo, 104-8560, Japan.

E-mail address: tatsu@luke.ac.jp (A. Tasaki).

https://doi.org/10.1016/j.jseint.2024.03.003

(glenoid osseous lesion), which is defined as avulsed bone fragment in the anteroinferior part of the glenoid, may undergo bone remodeling if repaired on the glenoid.[6,11] Thus, a detailed evaluation of the glenoid morphology and bony Bankart lesion plays an essential role in determining the surgical technique.

Ideally, preoperative soft tissue and bone morphometry evaluations are performed using magnetic resonance imaging (MRI) and computed tomography (CT), respectively. These evaluations are conducted separately for traumatic anterior shoulder instability. Conventional MRI sequences use an echo time of a few milliseconds; thus, it is not possible to obtain signals from tissues with short T2 values and transverse relaxation times. Although the evaluation of the cortical bone is essential for determining the glenoid morphology, evaluating the cortical bone using MRI is difficult as the T2 value of the bone cortex is extremely small, and no signal is obtained using the conventional MRI sequence. CT examinations have been performed for bone evaluation; however, the radiation exposure associated with CT examinations may induce malignant diseases.[4] New imaging techniques, such as the T1-volumetric interpolated breath-hold examination sequence,[7,12] ultrashort echo time sequence,[8] and zero echo time (ZTE) sequence,[1,2,9,13] have been developed as bone cortex imaging techniques using MRI in recent years. Several studies have evaluated the glenoid morphology using the ZTE sequence;[2,9] however, no detailed study evaluating bony Bankart lesion has been reported. The use of ZTE MRI will aid in reducing radiation exposure and medical costs.

Therefore, this study aimed to evaluate the glenoid morphology and detect bony Bankart lesion in shoulders with anterior instability using ZTE MRI and compare the diagnostic accuracy of ZTE MRI with that of CT. It was hypothesized that ZTE MRI would be able to evaluate glenoid morphology with a diagnostic accuracy similar to that of CT, but its diagnostic ability for detecting bony Bankart lesion would be limited.

Materials and methods

This study was conducted in accordance with the Declaration of Helsinki, and ethical approval was obtained from the Institutional Review Board. Informed consent was obtained from all patients and relevant individuals prior to commencing the study. Patients with traumatic anterior instability of the shoulder who had undergone preoperative CT and MRI examinations at our institution between April 2019 and October 2021 were eligible for inclusion in this study. The exclusion criteria were as follows: (1) patients who declined participation in this study, (2) patients with a history of undergoing surgery on the ipsilateral shoulder, (3) patients with shoulder instability without traumatic injury, and (4) patients with CT and/or MRI images that were judged to be unsuitable for the measurements in this study. All patients underwent CT examinations using Aquilion ONE Prism (Canon Medical Systems, Tochigi, Japan), Revolution CT (GE Healthcare Japan, Tokyo, Japan), or Revolution CT Maxima (GE Healthcare Japan, Tokyo, Japan). The parameters for the CT examination were as follows: tube voltage, 120 kV; rotation speed, 0.5 rot/s; and slice thickness, 0.5 or 0.625 mm. All patients underwent MRI examinations using Discovery MR750w 3.0-T (GE Healthcare Japan, Tokyo, Japan) with a surface coil for the shoulder joint. The parameters for the ZTE sequence were as follows: slice thickness, 1.0 mm; field of view, 200 × 200 mm; matrix, 200; repetition time, 484 ms; echo time, 0.016 ms; flip angle, 1°; and acquisition time, 5 min 42 s. The images were corrected and inverted to create CT-like images. Three-dimensional (3D) images were created from CT-like images subsequently. The processing software used was Volume Viewer (version 13.0; GE Healthcare Japan).

Glenoid bone defects were measured by drawing a best-fit circle on the inferior two-thirds of the glenoid on en face view 3D CT and 3D ZTE images.[10] Similar to the 3D CT images, the 3D ZTE images were sufficiently clear to facilitate measurement using the best-fit circle method. The percentages of bone loss on 3D CT and 3D ZTE images were calculated, and the correlation between the 2 was evaluated. Two orthopedic surgeons (T.O. and M.M.) determined the percentage of bone loss independently to evaluate the reproducibility of the measurement of the percentage of bone loss. In addition, one orthopedic surgeon (T.O.) performed the measurements twice at an interval of at least 3 weeks between the measurements. The number of patients with bony Bankart lesion on CT and ZTE (3D and CT-like) images was also determined. The patients with bony Bankart lesion on CT images were divided into 2 groups based on the presence of bony Bankart lesion on 3D ZTE images or the presence of bony Bankart lesion on CT-like images. The longer diameter of the bone fragment on the 3D CT images was compared between the groups (Fig. 1).

Statistical analysis

The Shapiro-Wilk test was used to evaluate the normality of continuous variables. The Mann-Whitney U test was used to compare the 2 groups. Spearman's rank correlation coefficient was used to evaluate the correlation between the percentages of glenoid bone loss on 3D CT and 3D ZTE images. A power analysis was conducted subsequently. The intraclass correlation coefficient (ICC) was calculated to assess the reproducibility of the measurement of the percentage of glenoid bone loss. The sensitivity, specificity, and positive and negative predictive values were calculated to assess the diagnostic accuracy of CT-like and 3D ZTE images for detecting bony Bankart lesion, using CT as the gold standard. A P value of $< .05$ was considered statistically significant.

Results

Among the 47 shoulders with anterior instability that were subjected to CT and MRI examinations, including the ZTE sequence, between April 2019 and October 2021, 5 shoulders with a history of undergoing surgery on the ipsilateral shoulder and 6 shoulders with images that were deemed unsuitable for measurement were excluded. Thus, 36 shoulders of 36 patients (30 males and 6 females) were included in the final analysis. Nineteen right and 17 left shoulders were included in the study (Table I). Thirty-one of the 36 patients underwent surgery for shoulder joint instability, whereas the remaining 5 did not. The interval between the CT and MRI examinations was < 1 month in all cases. The median percentages of glenoid bone loss were 12.1% and 12.3% on the 3D CT and 3D ZTE images, respectively. The ICC (1, 1) for the measurement of the percentage of bone loss was 0.93 and 0.92 for CT and ZTE, respectively. The ICC (2, 1) for the measurement of the percentage of bone loss was 0.85 and 0.83 for CT and ZTE, respectively (Table I). The Spearman's rank correlation coefficient was 0.89 (95% confidence interval [CI]; 0.85-0.96, power = 1.00) (Fig. 2).

Bony Bankart lesion was detected in 18 (50%), 13 (36%), and 8 (22%) of the 36 shoulders on CT, 3D ZTE, and CT-like images, respectively (Fig. 3). There were no cases wherein the bony Bankart lesion was undetectable on CT images but was detectable on 3D ZTE. The overall diagnostic accuracy for the detection of bony Bankart lesion was 86.1% (95% CI; 75.5%-96.8%) and 72.2% (95% CI; 60.4%-84.0%) on CT and 3D ZTE images, respectively, with CT as the gold standard. Table II summarizes the diagnostic accuracy. No

Figure 1 Measurement of the long diameter of bony Bankart lesion on a 3D CT image. The measurement was performed on an en face view image. *3D CT*, 3-dimensional computed tomography.

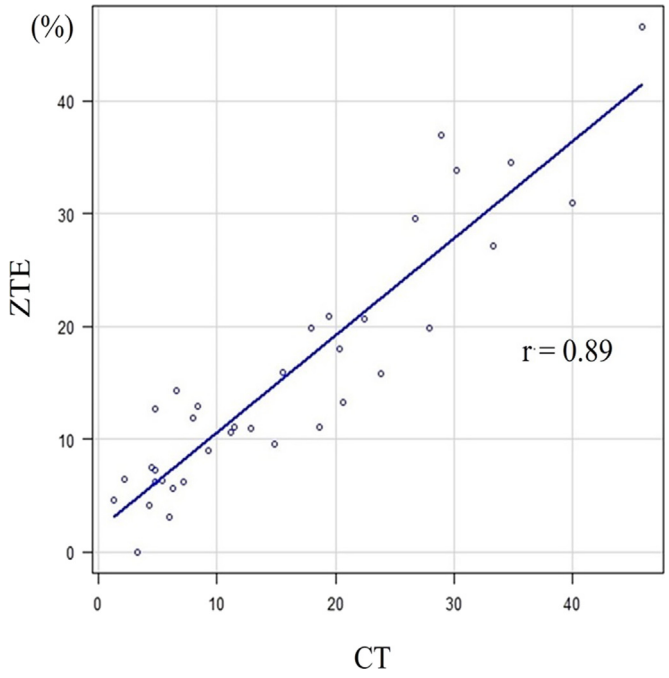

Figure 2 Correlation between the percentages of glenoid bone defect on CT and ZTE MRI. *CT*, computed tomography; *ZTE MRI*, zero echo time magnetic resonance imaging.

Table I
Patient characteristics and the rate of glenoid bone defect on CT and ZTE MRI.

Mean age at the time of MRI acquisition, y (range)	27.2 (16-59)
Sex, n	Male, 30; Female, 6
Laterality, n	Right, 19; Left, 17
Percentage of glenoid bone defect on CT, %	12.1 (1.3-45.9)*
Percentage of glenoid bone defect on ZTE MRI, %	12.3 (0-46.6)*

CT, computed tomography; *ZTE*, zero echo time; *MRI*, magnetic resonance imaging.
*Data are presented as median (range).

significant difference was observed between the groups with (median 15.1 mm, range 9.1-24.1 mm) and without (median 11.0 mm, range 4.8-37.7 mm) bony Bankart lesion on the 3D ZTE image in terms of the long diameter of the bone fragment on CT images ($P = .20$) (Fig. 4 and Table III). However, a significant difference was observed between the group with (median 15.3 mm, range 9.1-37.7 mm) and the group without (median 7.2 mm, range 4.8-10.3 mm) bony Bankart lesion on the CT-like image in terms of the long diameter of the bone fragment on CT images ($P < .01$) (Fig. 5 and Table III).

Discussion

The results of the evaluation of glenoid morphology and bony Bankart lesion using ZTE MRI in this study revealed that ZTE shows high reproducibility in the evaluation of glenoid bone loss. Moreover, no significant difference in the measurements was observed compared with those of CT. However, the diagnostic accuracy of ZTE was inferior to that of CT for detecting bony Bankart lesion. Moreover, bone fragments of < 9 mm were not detectable on CT-like images.

The ZTE sequence, a novel imaging technique characterized by a very short echo time, can image tissues with low T2 values, such as the bone cortex. ZTE sequence has the advantages of a relatively short acquisition time and a high signal-to-noise ratio. Previous studies on the evaluation of bone morphology in the skull,[13] hip joint,[1] and shoulder joint[2,9] using the ZTE sequence have reported good evaluation performance. Breighner et al reported a good intermodality agreement between ZTE and CT for the evaluation of Bankart lesion.[2] Similarly, de Mello et al reported that ZTE showed good interobserver reliability in the evaluation of glenoid width. Moreover, it was comparable with CT in this regard.[9] ZTE showed good interobserver and intraobserver reliability in the present study. In addition, a high correlation was also observed between the ZTE and CT measurements (r = 0.89), suggesting that ZTE is suitable for evaluating glenoid bone loss in clinical settings.

In contrast, the performance of ZTE was found to be inferior to that of CT for the detection of bony Bankart lesion. Among the cases with bony Bankart lesion on CT images, bony Bankart lesion was detected on the CT-like images in 72.2% of cases. In contrast, bony Bankart lesion was detected on the 3D ZTE images in only 44.4% of cases. The distribution of the long diameter of the bone fragments on CT-like and 3D ZTE images can be clearly visualized on the box-and-whisker plots presented in Figs. 4 and 5. The distributions of the long diameter of the bone fragments on CT-like images can be clearly differentiated between the groups with and without bony Bankart lesions (Fig. 5). The long diameter of the bone fragment on 3D CT was > 10 mm in 12 of the 13 cases with bony Bankart lesion detectable on CT-like images. The diameter was < 10 mm in 4 of the 5 cases with undetectable bony Bankart lesion. The diagnostic accuracy of CT-like images for detecting bony Bankart lesion is related to the bone fragment size. The cut-off value appears to be approximately 10 mm. Other possible factors include the difference in slice thickness between CT and MRI and the possibility that the signal intensity of MRI may decrease owing to changes in the properties of the bone fragment over time. The presence of bony Bankart lesion must be determined preoperatively as their repair can lead to favorable remodeling of the glenoid and postoperative outcomes. However, as bony Bankart lesion may be overlooked during preoperative evaluation using 3D ZTE alone, CT examinations should also be performed.

The diagnostic accuracy of 3D ZTE for detecting bony Bankart lesion was inferior to that of CT and CT-like images. 3D ZTE images

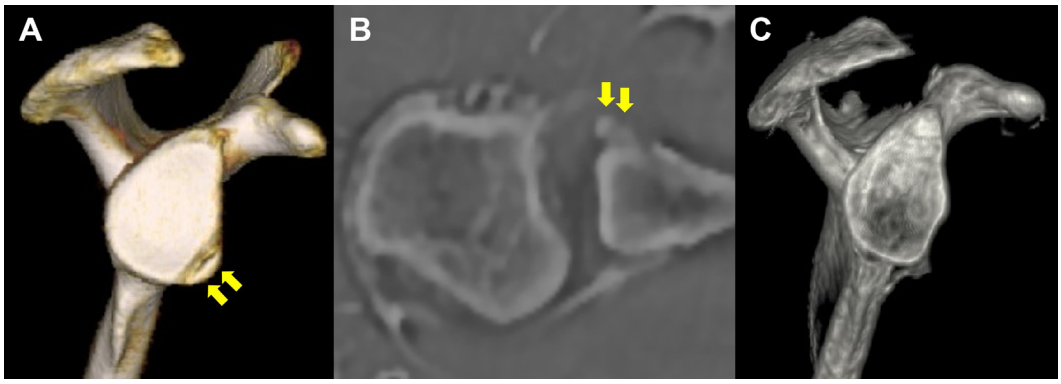

Figure 3 Representative case of a 20-year-old male with a bony Bankart lesion ⬇ detectable on CT and CT-like images but not on the 3D ZTE images of the right shoulder. (**A**) 3D CT image. (**B**) CT-like image. (**C**) 3D ZTE image. *CT*, computed tomography; *ZTE MRI*, zero echo time magnetic resonance imaging; *3D*, 3-dimentional.

Table II
Diagnostic accuracies of CT-like images and 3D ZTE images for detecting bony Bankart lesion.

	Sensitivity (%)	Specificity (%)	PPV (%)	NPV (%)	Overall accuracy (%)
CT-like images	72.2 (46.5-90.3)	100 (81.5-100)	100 (75.3-100)	78.3 (56.3-92.5)	86.1 (75.5-96.8)
3D ZTE images	44.4 (21.5-69.2)	100 (81.5-100)	100 (63.1-100)	64.3 (44.1-81.4)	72.2 (60.4-84.0)

CT, computed tomography; *ZTE*, zero echo time; *3D*, 3-dimensional; *PPV*, positive predictive value; *NPV*, negative predictive value.
Note. Values are presented with 95% confidence intervals.

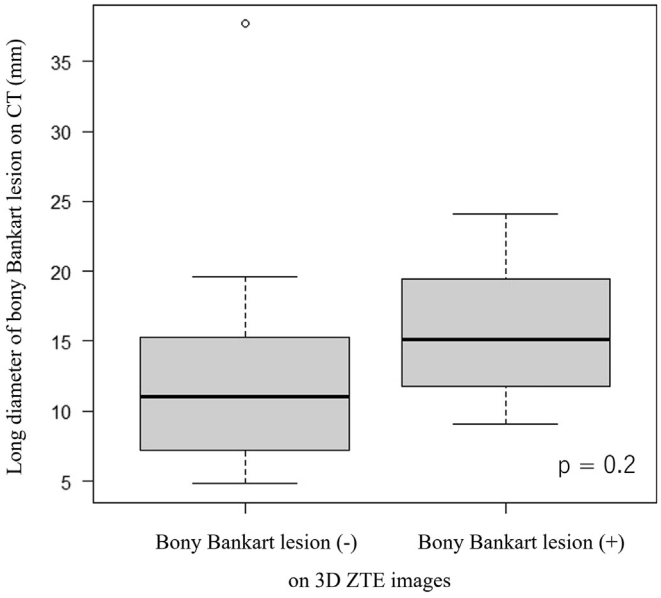

Figure 4 Box-and-whisker plot of the long diameter of the bony Bankart lesion on CT in the group with and without bony Bankart lesion on 3D ZTE images. *CT*, computed tomography; *3D*, 3-dimentional; *ZTE MRI*, zero echo time magnetic resonance imaging.

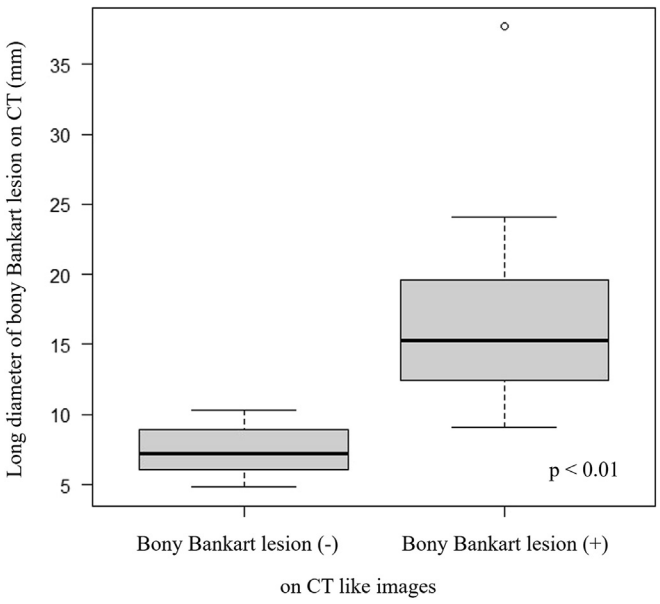

Figure 5 Box-and-whisker plot of the long diameter of the bony Bankart lesion on CT in the group with and without bony Bankart lesion on CT-like images. *CT*, computed tomography.

Table III
Long diameter of the bony Bankart lesion on CT in the groups with and without bony Bankart lesion on 3D ZTE and CT-like images.

	Bony Bankart lesion (+)	Bony Bankart lesion (−)	*P* value
3D ZTE images (%)	15.1 (9.1-24.1)*	11.0 (4.8-37.7)*	.20
CT-like images (%)	15.3 (9.1-37.7)*	7.2 (4.8-10.3)*	<.01

CT, computed tomography; *3D*, 3-demensional; *ZTE*, zero echo time.
*Data are presented as median (range).

were created from CT-like images by a radiologist by manually adding and deleting pixels using specialized image-processing software. It is possible that bony Bankart lesion is difficult to diagnose due to inappropriate recognition threshold settings of the image processing software and human error in the creation of the 3D image. Thus, it is necessary to identify optimal software settings and improve the software functionality to reduce manual labor and enhance the diagnostic ability of 3D ZTE for detecting bony Bankart lesion.

This study had certain limitations. First, analysis of the factors that affect diagnostic accuracy, such as the bone fragment size, interval between injury and MRI examination, and experience with the image processor, was difficult as the sample size was small, particularly the number of cases with bony Bankart lesion. Furthermore, the models and slice thickness of the CT slices were not uniform.

Conclusion

ZTE MRI demonstrated high reproducibility for the evaluation of glenoid bone defect in shoulders with anterior instability. Although no significant difference in the measurement was observed compared with that on CT, the ability of ZTE MRI to delineate bone Bankart lesion remains limited.

Disclaimers:

Funding: This work was partly supported by JSPS KAKENHI, Japan (Grant Number 21K07712).
Conflicts of interest: The authors, their immediate families, and any research foundation with which they are affiliated have not received any financial payments or other benefits from any commercial entity related to the subject of this article.

References

1. Breighner RE, Bogner EA, Lee SC, Koff MF, Potter HG. Evaluation of osseous morphology of the hip using zero echo time magnetic resonance imaging. Am J Sports Med 2019;47:3460-8. https://doi.org/10.1177/0363546519878170.
2. Breighner RE, Endo Y, Konin GP, Gulotta LV, Koff MF, Potter HG. Zero echo time imaging of the shoulder: enhanced osseous detail by using MR imaging. Radiology 2018;286:960-6. https://doi.org/10.1148/radiol.2017170906.
3. Burkhart SS, De Beer JF. Traumatic glenohumeral bone defects and their relationship to failure of arthroscopic Bankart repairs. Arthroscopy 2000;16:677-94.
4. De González AB, Darby S. Risk of cancer from diagnostic X-rays: estimates for the UK and 14 other countries. Lancet 2004;363:345-51. https://doi.org/10.1016/S0140-6736(04)15433-0.
5. Itoi E, Lee SB, Berglund LJ, Berge LL, An KN. The effect of a glenoid defect on anteroinferior stability of the shoulder after Bankart repair: a cadaveric study. J Bone Joint Surg Am 2000;82:35-46.
6. Kitayama S, Sugaya H, Takahashi N, Matsuki K, Kawai N, Tokai M, et al. Clinical outcome and glenoid morphology after arthroscopic repair of chronic osseous bankart lesions. J Bone Joint Surg Am 2014;97:1833-43. https://doi.org/10.2106/JBJS.N.01033.
7. Koh E, Walton ERJ, Watson P. Vibe MRI: an alternative to CT in the imaging of sports-related osseous pathology? Br J Radiol 2018;91:20170815. https://doi.org/10.1259/bjr.20170815.
8. Ma YJ, West J, Nazaran A, Cheng X, Hoenecke H, Du J, et al. Feasibility of using an inversion-recovery ultrashort echo time (UTE) sequence for quantification of glenoid bone loss. Skeletal Radiol 2018;47:973-80. https://doi.org/10.1007/s00256-018-2898-4.
9. de Mello RAF, Ma Y, Ashir A, Jerban S, Hoenecke H, Carl M, et al. Three-dimensional zero echo time magnetic resonance imaging versus 3-dimensional computed tomography for glenoid bone assessment. Arthroscopy 2020;36:2391-400. https://doi.org/10.1016/j.arthro.2020.05.042.
10. Sugaya H, Moriishi J, Dohi M, Kon Y, Tsuchiya A. Glenoid rim morphology in recurrent anterior glenohumeral instability. J Bone Joint Surg 2003;85:878-84. https://doi.org/10.2106/00004623-200305000-00016.
11. Tasaki A, Morita W, Nozaki T, Yonekura Y, Saito M, Phillips BB, et al. Arthroscopic bankart repair and open bristow procedure in the treatment of anterior shoulder instability with osseous glenoid lesions in collision athletes. Orthop J Sports Med 2021;9:23259671211008274. https://doi.org/10.1177/23259671211008274.
12. Tian CY, Shang Y, Zheng ZZ. Glenoid bone lesions: comparison between 3D VIBE images in MR arthrography and nonarthrographic MSCT. J Magn Reson Imaging 2012;36:231-6. https://doi.org/10.1002/jmri.23622.
13. Wiesinger F, Sacolick LI, Menini A, Kaushik SS, Ahn S, Veit-Haibach P, et al. Zero TE MR bone imaging in the head. Magn Reson Med 2016;75:107-14. https://doi.org/10.1002/mrm.25545.